IEEE Access
Multidisciplinary | Rapid Review | Open Access Journal

Received October 24, 2017, accepted November 10, 2017, date of publication November 29, 2017,
date of current version February 14, 2018.

Digital Object Identifier 10.1109/ACCESS.2017.2778427

Impedance-Based Fault Location Method for Four-Wire Power Distribution Networks

RAHMAN DASHTI[1], MOHAMMAD DAISY[1], (Member, IEEE), HAMID REZA SHAKER[2], (Member, IEEE), AND MARYAMSADAT TAHAVORI[2]

[1]Electrical Engineering Department, Faculty of Engineering, Persian Gulf University, Bushehr 7516913817, Iran
[2]Center for Energy Informatics, The Maersk Mc-Kinney Moller Institute, University of Southern Denmark, 5230 Odense, Denmark

Corresponding author: Hamid Reza Shaker (hrsh@mmmi.sdu.dk)

ABSTRACT Fault location techniques play an essential role in system recovery and repair. Therefore, numerous methods have been presented for fault location in power transmission and distribution networks. The contribution of this paper is to extend the state-of-art impedance-based fault location methods to support four-wire power distribution. To make this possible an algorithm is developed. The method is obtained using the principles of circuit theory and overcomes the challenges which prevent the use of most fault location methods for distribution networks in practice. This paper presents the detailed equations which are used in the algorithm and how they are obtained. The satisfactory performance of the algorithm is confirmed with numerical examples using MATLAB software.

INDEX TERMS Distribution networks, fault locating, fault estimation section, impedance-based fault locating, π line model.

I. INTRODUCTION

Distribution networks distribute the power that has already entered the cities by transmission networks among consumers. One of the important points associated to the power lines (transmission and distribution) is the problem of divulging fault in these lines. This issue is inevitable. Divulging fault can result in difficulties such as damaging network equipment, interruption in providing service for consumers, making the network unstable and finally, decreasing the network reliability. All these problems can impose financial loss to consumers, power plants and companies [1]–[3].

Four-wire three-phase systems are widely used in distribution networks since they have higher sensitivity for protection and better fault removal capabilities compared to the three-wire three-phase counterparts. The ground wire has current due to the loads imbalance in the three phase as well as the nonlinear characteristic of the loads. Even a significant imbalance in some feeders causes that the ground wire current to be higher than other phases. The ground wire in load distribution programs and available fault analysis is usually combined with wire of phases. Since the ground wire does not appear clearly in equations, its current and voltage will be unavailable. In some applications, such as fault analysis, power quality, safety issues, etc., it is very important to know the voltage and current of the ground wire. Therefore, an algorithm that can provide the location of the fault with respect to the ground wire is needed [4].

According to the conducted studies, evolutionary flow of recognizing fault location can be taken into account in the form of subscribers contact and expressing their observations, presence of the operators on the spot, the use of off-line and real-time fault finders. The literature has been focused on the real-time strategies and various methods for fault location in the transmission networks have been proposed. These techniques, however, do not thoroughly consider the attributes of distribution systems (unbalanced operation, presence of intermediate loads, laterals/sub laterals, and time varying load profile), which significantly affect the methods performance [5], [6].

Several methods have been proposed for fault distance detection in transmission lines. However, the significant structural differences of the distribution network and the transmission line have caused that the methods presented for transmission lines cannot be used for fault location in the distribution networks. Therefore, methods such as impedance, travelling waves and artificial intelligence were presented in such a way that they can solve the problem of locating faults in the distribution networks. These methods however still suffer from some problems. Travelling waves-based methods have problems such as the need for a high sampling fre-

FIGURE 1. Single-line diagram of distribution network.

quency, a complex structure, and the need for a data bank. The need for a large and accurate data bank that should be updated with the smallest change in the network is among the problem of the artificial intelligence methods. This is in addition to its complex structure. Due to the above problems, presenting an efficient method is necessary that can accurately determine the location of the fault with proper accuracy. In distribution networks, mainly impedance-based fault location detection methods are used to determine the possible locations of faults according to simplicity in implementation, low cost, and the use of simple equations and calculations [7]–[9].

Fault analysis in four-wire distribution networks is discussed in [4]. The methodology for fault analysis is based on the generalized backward–forward technique and hybrid compensation short-circuits method. The methodology is generally used since it enables fault analysis in most of the existing distribution networks. While the presented method in [4] is interesting for fault detection, it does not provide results on fault location.

In this paper, we extend the state-of-art impedance methods to support four-wire distribution networks. We propose a fault location algorithm considering the fourth wire separately for four wire networks using π line model. The main specifications of distribution networks including sub branches, fault resistance, fault location, error start angle and type of the fault have been presented in the proposed algorithm.

II. THE PROPOSED METHOD FOR DETERMINING FAULT DISTANCE

Distribution network consists of different sections. Each section is a part of a distribution network which is located between two sequent nodes. Single-line diagram of each section has been shown in Fig. 1. In this part, π line model has been used for modeling of each section. The circuit diagram of each section is shown in the Fig. 2.

where:

S: sending bus

R: receiving bus

From voltage rule and Kirchhoff's current law, we have:

$$\begin{bmatrix} V_{abcn_m} \\ I_{abcn_m} \end{bmatrix} = \begin{bmatrix} d_l & -b_l \\ -c_l & a_l \end{bmatrix} \cdot \begin{bmatrix} V_{abcn_n} \\ I_{abcn_n} \end{bmatrix} \quad (1)$$

where:

V_{abcn_m}: Three-phase and neutral voltage at the end of study section.

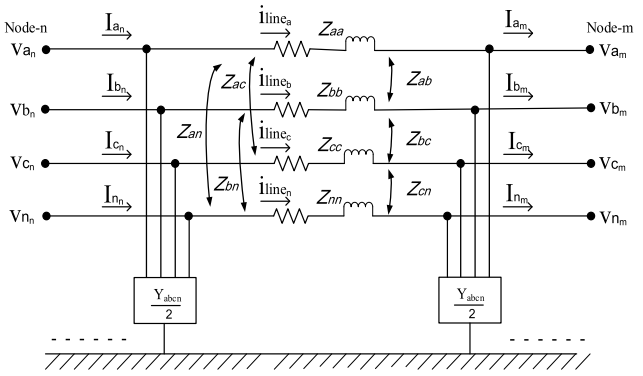

FIGURE 2. Four wire exact line segment model.

I_{abcn_m}: Three-phase and neutral current at the end of study section.

V_{abcn_n}: Three-phase and neutral voltage at the beginning of study section.

I_{abcn_n}: Three-phase and neutral current at the beginning of study section.

According to [10]:

$$a_l = d_l = I + 0.5 \cdot l^2 \cdot Z_{abcn} \cdot Y_{abcn} \quad (2)$$

$$b_l = l \cdot Z_{abcn} \quad (3)$$

$$c_l = l \cdot Y_{abcn} + 0.25 \cdot l^3 \cdot Y_{abcn} \cdot Z_{abcn} \cdot Y_{abcn} \quad (4)$$

where:

Z_{abcn}: impedance matrix of study section (per length unit).

Y_{abcn}: admittance matrix of study section (per length unit).

Equation (1) can be rewritten for fault point voltage (fault in the distance of x kilometer from the beginning of the line) as follows:

$$V_F = d_x \cdot V_S - b_x \cdot I_S \quad (5)$$

Where in this equation, V_s and I_s are voltage and current at the beginning of section, V_F is the voltage of fault point and variables d_x and b_x are obtained by replacing x instead of l in (2) and (3). As it is observed from (5), the shunt admittance is considered in fault location via d_x and it will be affected, effectively. All types of faults are divided into two groups of faults: the ground faults (single phase to ground, two-phase to ground and three- phase to ground) and phase faults (two phase to each other). Suggested algorithms for fault locating for these two groups will be presented separately as follows.

A. GROUND FAULTS

Generally, ground faults are shown in Fig. 3. Fault point voltage of different phases is shown in (6) that is depended on fault impedances and fault currents. Using this equation, voltage of fault point in the phase k (k=*a, b and c*) can be calculated by (7).

where: ILn: the phase current flow from load point to the fault point. $I_{i(a,b\text{ or }c)}$: the phase current flow from the upstream fault point to that. $Il_{i(a,b\text{ or }c)}$: the phase current from the downstream fault point to that. $I_{Fi(a,b\text{ or }c)}$: injection fault

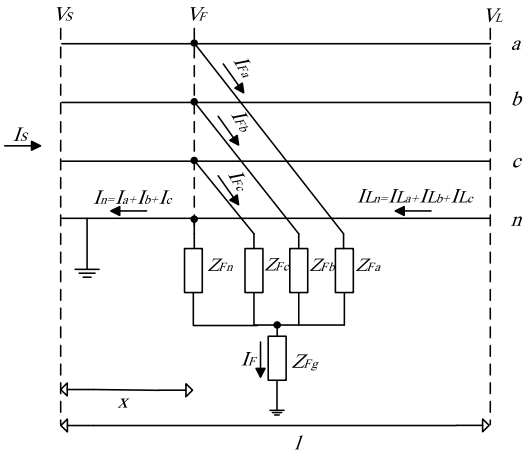

FIGURE 3. Distribution line subjected to a general ground fault.

current from phase i. I_n: neutral wire fallowing current from the fault point to the beginning of section.

$$\begin{bmatrix} V_{F_a} \\ V_{F_b} \\ V_{F_c} \\ V_{F_n} \end{bmatrix} = \begin{bmatrix} Z_{F_a}+Z_{F_g} & Z_{F_g} & Z_{F_g} & Z_{F_g} \\ Z_{F_g} & Z_{F_b}+Z_{F_g} & Z_{F_g} & Z_{F_g} \\ Z_{F_g} & Z_{F_g} & Z_{F_c}+Z_{F_g} & Z_{F_g} \\ Z_{F_g} & Z_{F_g} & Z_{F_g} & Z_{F_n}+Z_{F_g} \end{bmatrix} \cdot \begin{bmatrix} I_{F_a} \\ I_{F_b} \\ I_{F_c} \\ I_{Fn} \end{bmatrix} \tag{6}$$

$$V_{F_k} = Z_{F_k} \cdot I_{F_k} + Z_{F_g} \cdot I_F \tag{7}$$

where:

$$I_F = I_{F_a} + I_{F_b} + I_{F_c} + I_{F_n} \tag{8}$$

Both (5) and (6) describe fault point voltage. By comparing each faulty phase of k using these two equations and substituting the (2) and (3) in (5), we obtain:

$$V_{F_k} = Z_{F_k} \cdot I_{F_k} + Z_{F_g} \cdot I_F = V_{S_k} + x^2 \cdot 0.5 \cdot M_k - x \cdot N_k \tag{9}$$

Where the coefficients M_K and N_K are defined as follow:

$$\begin{bmatrix} M_a \\ M_b \\ M_c \\ M_n \end{bmatrix} = \begin{bmatrix} Z_{aa} & Z_{ab} & Z_{ac} & Z_{an} \\ Z_{ba} & Z_{bb} & Z_{bc} & Z_{bn} \\ Z_{ca} & Z_{cb} & Z_{cc} & Z_{cn} \\ Z_{na} & Z_{nb} & Z_{nc} & Z_{nn} \end{bmatrix} \cdot \begin{bmatrix} Y_{aa} & Y_{ab} & Y_{ac} & Y_{an} \\ Y_{ba} & Y_{bb} & Y_{bc} & Y_{bn} \\ Y_{ca} & Y_{cb} & Y_{cc} & Y_{cn} \\ Y_{na} & Y_{nb} & Y_{nc} & Y_{nn} \end{bmatrix} \cdot \begin{bmatrix} V_{S_a} \\ V_{S_b} \\ V_{S_c} \\ V_{S_n} \end{bmatrix} \tag{10}$$

$$\begin{bmatrix} N_a \\ N_b \\ N_c \\ N_n \end{bmatrix} = \begin{bmatrix} Z_{aa} & Z_{ab} & Z_{ac} & Z_{an} \\ Z_{ba} & Z_{bb} & Z_{bc} & Z_{bn} \\ Z_{ca} & Z_{cb} & Z_{cc} & Z_{cn} \\ Z_{na} & Z_{nb} & Z_{nc} & Z_{nn} \end{bmatrix} \cdot \begin{bmatrix} I_{S_a} \\ I_{S_b} \\ I_{S_c} \\ I_{S_n} \end{bmatrix} \tag{11}$$

By separating the real and imaginary parts of (9), (12) and (13) are determined. Most of the time the fault impedances (Z_{F_a}, Z_{F_b} and Z_{F_c}) are assumed to be pure resistance. Therefore, the second term is zero.

$$\begin{aligned} \mathrm{Re}\{V_{F_k}\} &= R_{F_k} \cdot I_{F_{k_r}} + R_{F_g} \cdot I_{F_r} - X_{F_g} \cdot I_{F_i} \\ &= V_{S_{k_r}} + x^2 \cdot 0.5 \cdot M_{k_r} - x \cdot N_{k_r} = T_{k_r} \end{aligned} \tag{12}$$

$$\begin{aligned} \mathrm{Im}\{V_{F_k}\} &= R_{F_k} \cdot I_{F_{k_i}} + R_{F_g} \cdot I_{F_i} + X_{F_g} \cdot I_{F_r} \\ &= V_{S_{k_i}} + x^2 \cdot 0.5 \cdot M_{k_i} - x \cdot N_{k_i} = T_{k_i} \end{aligned} \tag{13}$$

In the above equations, r and i are real and imaginary parts of variables, respectively. Based on the (12) and (13), R_{F_k} can be computed using (14) and (15). By removing the R_{F_k} from the above equations, (16) is obtained:

$$R_{F_k} = \frac{1}{I_{F_{k_r}}} \cdot \left[T_{k_r} - R_{F_g} \cdot I_{F_r} + X_{F_g} \cdot I_{F_i}\right] \tag{14}$$

$$R_{F_k} = \frac{1}{I_{F_{k_i}}} \cdot \left[T_{k_i} - R_{F_g} \cdot I_{F_i} - X_{F_g} \cdot I_{F_r}\right] \tag{15}$$

$$\begin{aligned} R_{F_g} \cdot \left[-\frac{I_{F_r}}{I_{F_{k_r}}} + \frac{I_{F_i}}{I_{F_{k_i}}}\right] + X_{F_g} \cdot \left[\frac{I_{F_i}}{I_{F_{k_r}}} + \frac{I_{F_r}}{I_{F_{k_i}}}\right] \\ + \left[\frac{T_{k_r}}{I_{F_{k_r}}} - \frac{T_{k_i}}{I_{F_{k_i}}}\right] = 0 \end{aligned} \tag{16}$$

By multiplying $(-I_{F_{k_r}} \cdot I_{F_{k_i}})$ to (16) the following equation can be concluded:

$$\begin{aligned} R_{F_g} \cdot \mathrm{Im}\left\{I_{F_k} \cdot I_F^*\right\} - X_{F_g} \cdot \mathrm{Re}\left\{I_{F_k} \cdot I_F^*\right\} \\ + \left[T_{k_r} \cdot I_{F_{k_i}} - T_{k_i} \cdot I_{F_{k_r}}\right] = 0 \end{aligned} \tag{17}$$

For the ground faults such as single phase to ground, two-phase to ground, and three- phase to ground, (17) is re-written in the following form.

$$\begin{aligned} R_{F_g} \cdot \mathrm{Im}\left\{I_F \cdot I_F^*\right\} - X_{F_g} \cdot \mathrm{Re}\left\{I_F \cdot I_F^*\right\} \\ + \sum_{k \in \Omega_k} \left[T_{k_r} \cdot I_{F_{k_i}} - T_{k_i} \cdot I_{F_{k_r}}\right] = 0 \end{aligned} \tag{18}$$

The first term of (18) is imaginary part of $|I_F|^2$ which is equal to zero. The reason is that, it is a real number and imaginary part of a real number is zero (as it can be seen in (19)). Since fault impedance usually is assumed as resistance, the second term will be also zero. Therefore, for the ground faults, (18) is converted to (20).

$$\mathrm{Im}\left\{I_F \cdot I_F^*\right\} = \mathrm{Im}\left\{|I_F|^2\right\} = 0 \tag{19}$$

$$\sum_{k \in \Omega_k} \left[T_{k_r} \cdot I_{F_{k_i}} - T_{k_i} \cdot I_{F_{k_r}}\right] = 0 \tag{20}$$

By substituting (12) and (13) in (20), (21) is extracted which is a second order algebraic equation of fault distance:

$$\begin{aligned} x^2 \cdot \left[0.5 \cdot \sum_{k \in \Omega_k} \mathrm{Im}\left\{M_k \cdot I_{F_k}^*\right\}\right] - x \cdot \left[\sum_{k \in \Omega_k} \mathrm{Im}\left\{N_k \cdot I_{F_k}^*\right\}\right] \\ + \left[\sum_{k \in \Omega_k} \mathrm{Im}\left\{V_{S_k} \cdot I_{F_k}^*\right\}\right] = 0 \end{aligned} \tag{21}$$

This equation has been determined for all the ground faults (single phase, two-phase, and three-phase to ground). When the fault happens, the fault distance is determined using voltage and the current at the beginning of the section and the proposed impedance-based technique.

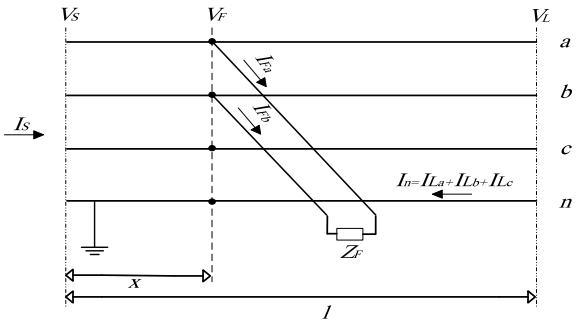

FIGURE 4. Line-to-line fault model.

B. PHASE FAULTS

Fig. 4 presents phase faults, where phase a and phase b are connected to each other with fault impedance Z_F. Based on Fig. 4, output current from the phase a toward the phase b and the voltage of fault point can be written as (22) and (23-a). Additionally, by substituting (2) and (3) in (5), the faulted point voltage at phase a and b can be determined (23-b) and (23-c).

$$I_{F_a} = -I_{F_b} \tag{22}$$

$$\begin{cases} V_{F_a} = V_{F_b} + Z_F \cdot I_{F_a} & (a) \\ V_{F_a} = V_{S_a} + x^2 \cdot 0.5 \cdot M_a - x \cdot N_a & (b) \\ V_{F_b} = V_{S_b} + x^2 \cdot 0.5 \cdot M_b - x \cdot N_b & (c) \end{cases} \tag{23}$$

Let's assume that Z_F is pure resistance. By separating the real and imaginary parts of (23-a), the two below equations are computed.

$$\begin{aligned} R_F \cdot I_{F_{a_r}} &= x^2 \cdot 0.5 \cdot \left(M_{a_r} - M_{b_r}\right) \\ &\quad - x \cdot \left(N_{a_r} - N_{b_r}\right) + \left(V_{S_{a_r}} - V_{S_{b_r}}\right) \end{aligned} \tag{24}$$

$$\begin{aligned} R_F \cdot I_{F_{a_i}} &= x^2 \cdot 0.5 \cdot \left(M_{a_i} - M_{b_i}\right) \\ &\quad - x \cdot \left(N_{a_i} - N_{b_i}\right) + \left(V_{S_{a_i}} - V_{S_{b_i}}\right) \end{aligned} \tag{25}$$

Then by removing Z_F, (26) is determined for phase faults location

$$\begin{aligned} x^2 \cdot 0.5 \cdot &\left[\frac{M_{a_i} - M_{b_i}}{I_{F_{a_i}}} - \frac{M_{a_r} - M_{b_r}}{I_{F_{a_r}}}\right] - x \\ &\cdot \left[\frac{N_{a_i} - N_{b_i}}{I_{F_{a_i}}} - \frac{N_{a_r} - N_{b_r}}{I_{F_{a_r}}}\right] \\ &+ \left[\frac{V_{S_{a_i}} - V_{S_{b_i}}}{I_{F_{a_i}}} - \frac{V_{S_{a_r}} - V_{S_{b_r}}}{I_{F_{a_r}}}\right] = 0 \end{aligned} \tag{26}$$

Equation (27) is obtained by multiplying $(I_{F_{a_r}} \cdot I_{F_{a_i}})$ to (26). This equation is second order algebraic equation of fault distance.

$$\begin{aligned} x^2 \cdot 0.5 \cdot \mathrm{Im}\left\{(M_a - M_b) \cdot I_{F_a}^*\right\} - x \cdot \mathrm{Im}\left\{(N_a - N_b) \cdot I_{F_a}^*\right\} \\ + \mathrm{Im}\left\{\left(V_{S_a} - V_{S_b}\right) \cdot I_{F_a}^*\right\} = 0 \end{aligned} \tag{27}$$

Equation (27) has been presented for two-phase faults between a and b. Similar equations can be written for two-phase faults between h and k:

$$\begin{aligned} x^2 \cdot 0.5 \cdot \mathrm{Im}\left\{(M_h - M_k) \cdot I_{F_h}^*\right\} - x \cdot \mathrm{Im}\left\{(N_h - N_k) \cdot I_{F_h}^*\right\} \\ + \mathrm{Im}\left\{\left(V_{S_h} - V_{S_k}\right) \cdot I_{F_h}^*\right\} = 0 \end{aligned} \tag{28}$$

C. DETERMINING THE PHYSICALLY CORRECT SOLUTION

The proposed fault location equations are second-order polynomials in x, the fault distance. Therefore, in each iteration of the previously described algorithm, two new fault distances are obtained. Only one of the solutions is real fault location. The other solution is mathematical answer and does not have a physical meaning. Selecting the correct answer is very critical. The answer with the following conditions is selected as the correct answer:

- Correct answer should be a real and positive number.
- Its value should be less than the length of evaluated section.

Studies show that just one of the answers from the (21) or (28) satisfies the above-mentioned conditions.

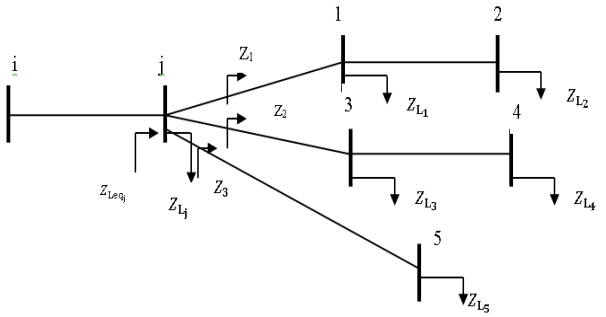

FIGURE 5. Single-line diagram of sample network.

III. ALGORITHM OF FAULT LOCATING FOR DISTRIBUTION NETWORKS

A. DETERMINING EQUIVALENT LOAD AT THE END OF EACH SECTION

In previous section, the proposed technique for fault location has been presented. The voltage and current at the beginning of the section and load data at the end of the section are assumed to be known in section II. However currents and voltages are measurable only at the beginning of the feeder in distribution networks. In the following, different methods have been presented for calculating impedance of equivalent load at the end of each section and also for calculating the voltage and current at the beginning of each section. Whereas the fault has happened in section ij (see Fig. 5) which is between nodes i and j, it is necessary to find impedance of

equivalent load at the end of this section. Equation (29) is used to obtained equivalent impedance.

$$Z_{Leq_j} = \left(Z_1^{-1} + Z_2^{-1} + Z_3^{-1} + Z_{L_j}^{-1}\right)^{-1} \tag{29}$$

To determine each of impedances z_1, z_2 and z_3, the observed equivalent impedance of *jth* node is computed. To find these impedances, series and parallel of loads impedance and lines impedance have been used. For having a higher precision, π line model has been used for each section. By using (30), (31) and (32) the equivalent impedance of each section which is connected to the node j is determined (see Fig. 5).

$$Y_1 = \left(\left[\left(\left(Z_{L_2}^{-1} + \frac{Y'_{12}}{2}\right)^{-1} + Z'_{12}\right)^{-1} + \frac{Y'_{12}}{2} + Z_{L_1}^{-1} + \frac{Y'_{j1}}{2}\right]^{-1} + Z'_{j1}\right)^{-1} + \frac{Y'_{j1}}{2} \tag{30}$$

$$Y_2 = \left(\left[\left(\left(Z_{L_4}^{-1} + \frac{Y'_{34}}{2}\right)^{-1} + Z'_{34}\right)^{-1} + \frac{Y'_{34}}{2} + Z_{L_3}^{-1} + \frac{Y'_{j3}}{2}\right]^{-1} + Z'_{j3}\right)^{-1} + \frac{Y'_{j3}}{2} \tag{31}$$

$$Y_3 = \left(\left(Z_{L_5}^{-1} + \frac{Y'_{j5}}{2}\right)^{-1} + Z'_{j5}\right)^{-1} + \frac{Y'_{j5}}{2} \tag{32}$$

$$Z_1 = Y_1^{-1}, \quad Z_2 = Y_2^{-1}, \; Z_3 = Y_3^{-1} \tag{33}$$

B. DETERMINING VOLTAGE AND CURRENT AT THE BEGINNING OF EACH SECTION

To be able to use the proposed technique in part II of this paper, the voltage and current at the beginning of the section are required to be known or determined. To determine the voltage and current the recorded data from the voltage and the current at the beginning of the feeder is used. We know that each node is situated on the downstream of the first node of the feeder. Therefore, the voltage on the downstream node V_{k_j} and input current of this node from previous node $V_{k_{ij}}$ can be calculated via (34) and (35). Let's assume that in Fig. 5, the voltage and current at the beginning of section $j-1$ (V_{S_j}, I_{S_j}) should be calculated. The existed voltages and currents at the beginning of section $i-j$ can be used to find V_{S_j}, I_{S_j}. In this case V_{k_j} is equal to V_{S_j} and is obtained by using (34) and input current of node j is obtained by using (35):

$$V_{k_j} = V_{S_k} + l_{k_j}^2 \cdot 0.5 \cdot M_k - l_{k_j} \cdot N_k \tag{34}$$

$$I_{k_{ij}} = -c_{l_{kj}} \cdot V_{F_k} + a_{l_{kj}} \cdot I_{F_k} \tag{35}$$

The currents of different branches and loads which are connected to node j are required to find output current from node j to node[1] ($I_{S_{j-1}}$, (36)).

$$I_{S_{j-1}} = I_{k_{ij}} - I_{th_{j-3,5}} \tag{36}$$

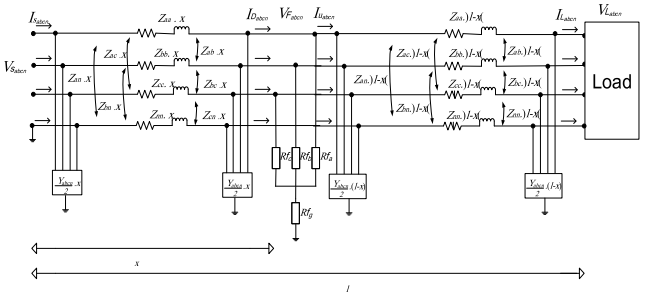

FIGURE 6. Typical section of PDS with a fault at distance from sending node [9].

$I_{k_{ij}}$: The sum of all currents that pass over all sections and the loads which are connected to node j.

$I_{S_{j-1}}$: Output current of nod j towards node1.

$I_{th_{j-3,5}}$: The sum of output currents from node j to all branches except the branch *j-1*.

$$I_{th_{j-3,5}} = \left(Z_2^{-1} + Z_3^{-1} + Z_{L_j}^{-1}\right) \cdot V_{S_j} \tag{37}$$

C. FAULT LOCATION ALGORITHM FOR POWER DISTRIBUTION SYSTEM

1) Fault Identification
   In this step, different types of faults are recognized to separate them from each other (single phase to the ground, two-phase to the ground, two-phase to each other and three-phase to the ground). Diverse strategies can be found in the literature for recognition of the fault type. In this paper, the fault type is recognized by using relay information at the beginning of the feeder.
2) Determining equivalent load impedance at the end of each section, and voltage and current at the beginning of each section.
3) Load current (I_L) before and after the fault are considered to be equal. Output current from fault point to the end side of the section (I_U) is considered to be equal to (I_L).
4) The input current to fault point from upside (I_D) and output current from the first node of the sector (I_S) are assumed to be equal.
   Fig. 6 shows the location of different currents.
5) Equation (38) is used to determine fault current.

$$I_F = I_D - I_U \tag{38}$$

6) Based on the fault type, (21) or (28) is used to find fault location.
7) Has x been convergent?
   If yes, algorithm is stopped and the value x is printed, otherwise going to stage 8.
8) Determining location voltage or fault point by using (7)
9) Updating the currents I_D and I_U by using (39) and (40) and turning to stage three.

$$I_D = -c_x \cdot V_{S_k} + a_x \cdot I_{S_k} \tag{39}$$

$$I_U = \left[Z_{Total}^{-1} + 0.5 \cdot (l-x) \cdot Y_{abcn}\right] \cdot V_F \tag{40}$$

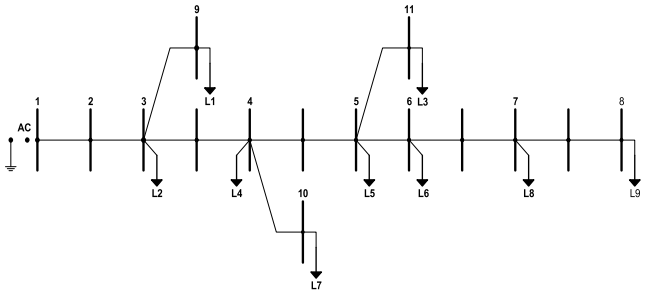

FIGURE 7. Single-line diagram of 11 nodes AL-1PL network [11].

$$Z_{Total} = (l - x) \cdot Z_{abcn} + \left[0.5 \cdot (l - x) \cdot Y_{abcn} + Z_{k+1}^{-1}\right]^{-1} \quad (41)$$

IV. THE RESULTS OF SIMULATION

A. INTRODUCING THE STUDIED NETWORKS

For assessing the execution of the proposed technique, the changed network of 11 nodes [11] AL-1PL is considered (see Fig. 7). The Simulink toolbox is used to simulate these networks. For modeling lines in different sections, model π has been used. The samples of three-phase voltage and current at the beginning of the feeder are measured and saved. Domain and voltage phase and three-phase current at the beginning of the feeder is required to perform the proposed algorithm. These parameters are found based on Fourier analysis. To find how precise fault locating is, (42) is used:

$$error\% = \frac{|x_{actual} - x_{calculated}|}{l_t} \times 100 \quad (42)$$

In this relation:

x_{actual}: Actual location of error. $x_{calculated}$: calculated error location. l_t: The length of the total feeder.

B. EVALUATING SUGGESTED METHOD OF FAULT LOCATING IN THE CHANGED NETWORK OF 11 NODES AL-1PL [11]

To check the proposed technique, first a single phase fault to the ground in the distance of half kilometer from the beginning of the feeder between nodes 1 and 2 is simulated. At this stage the simulation is done at fault resistance of 10Ω.

In this section, the voltage and the current at the beginning of each sector by using the saved information at the beginning of the feeder in error time is calculated. Then the method of finding distance of proposed fault for distribution network is performed. The error percent calculation for these conditions is 0.002%. The suggested technique also has been evaluated in two other fault locations between nodes 4 and 10 and between nodes 7 and 8. The obtained results show that the errors of the suggested method are %0.0153 and %0.024 respectively.

In the following the effects of different parameters on the precision of the proposed method is studied. Different factors such as fault resistance, fault distance, fault inception angle, and fault type have been taken into account.

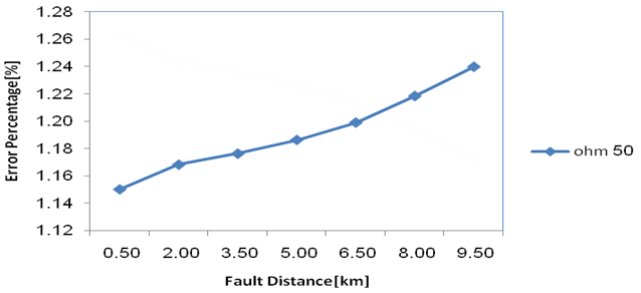

FIGURE 8. Error percentage of single phase to the ground.

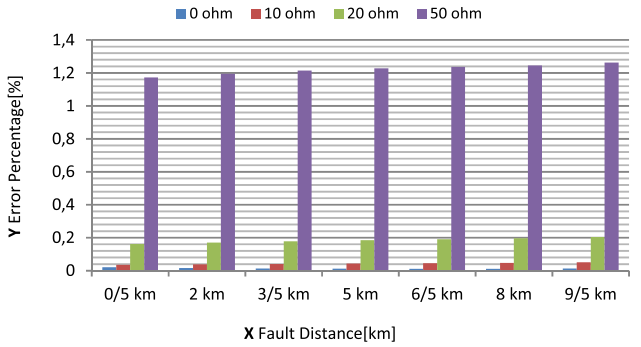

FIGURE 9. Error percentage in different fault locations with different fault resistances.

C. EFFECT OF DIFFERENT LOCATIONS OF FAULT ON PRECISION OF THE PROPOSED METHOD

To find how the suggested technique is sensitive to the fault occurrence locations, single phase fault to the ground in different locations has been simulated and the yielded results in proposed algorithm have been used. The accomplished results are presented in Fig. 8. Simulations for different distances of fault from the beginning of the feeder to the end, for single phase to the ground with fault resistance of 50Ω have been achieved. Based on the presented results in Fig. 8, it is observed that the effect of the error distance, on precision of suggested method is not considerable. Anyway the maximum error in this feeder would not be more than 1.263%.

D. EFFECT OF FAULT RESISTANCE ON THE PRECISION OF THE PROPOSED METHOD

Fault resistance is one of the critical parameters on the accuracy of the fault location algorithms. To evaluate the effect of fault resistance on proposed fault location technique, different simulations have been done at different resistances of fault (0, 10, 20, 50Ω). Since, the possibility of having single phase to the ground is more than other faults; in these simulations this type of fault has been considered. The results of these simulations are shown in Fig. 9. As the Fig. 9 show the error of the proposed technique in faults without resistance is not more than 0.021%, and for errors with fault resistance equal to 20Ω in different locations is less than 0.205%. Furthermore, from the results it can be found that error resistance on the proposed method doesn't have significant effect on faults near

TABLE 1. The effect of the fault type on the precision of the proposed method.

$R_F(\Omega)$	Fault Location (Node No.)	The type of the fault A-g	AB-g	AB	ABC-g
		Errors Percentage			
0	2	0.0067	0.1920	0.2307	0.0020
	10	0.0760	1.9800	2.3073	0.0153
	8	0.1460	3.7733	4.3920	0.0240
10	2	0.0507	0.2307	0.1600	0.0020
	10	0.0433	2.2760	2.2793	0.0153
	8	0.0360	4.2487	4.3980	0.0240
20	2	0.2047	0.2307	0.0633	0.0020
	10	0.1853	2.2967	2.0667	0.0153
	8	0.1620	4.3347	4.1887	0.0240
50	2	1.2627	0.2307	1.6093	0.0020
	10	1.2413	2.3033	0.5260	0.0153
	8	1.1733	4.3747	2.6560	0.0240

the beginning of the feeder. However, as branches and their lengths are increasing, the error for short connections at the end of the feeder will increase. And the maximum error in these simulations does not exceed more than 1.263 %.

E. THE EFFECT OF THE FAULT TYPE ON PRECISION OF THE PROPOSED METHOD

The proposed method in this part is table to find faults of different types in distribution networks. To find how the precision of the proposed technique is changing with the fault type in the studied network, different types of faults with different resistances and in different locations have been simulated that their results are presented in table (1). The results in table (1) show that the type of the faults does not have any effect on the precision of the presented technique.

F. THE EFFECT OF THE FAULT START ANGLE ON PRECISION OF THE PROPOSED METHOD

To see how sensitive the proposed method is on the fault start angle, various simulations have been done and the results are presented in table (2). These simulations have been done at, different fault start angles: 0°, 45°, 90° and 170°. For these simulations, fault resistance is assumed to be 10Ω. The presented results show that the proposed method is not sensitive to changes of the fault start angle.

G. EVALUATING THE UNBALANCED DISTRIBUTION EFFECT ON THE ACCURACY OF THE PROPOSED METHOD

The unbalanced load and feeder effects on the accuracy of proposed method have been evaluated in this section. For this investigation, the actual feeder system of Fig. 7 has been considered. 10 percent unbalance has been considered for all loads. In these simulations, the starting angle of the fault has been considered 45 degrees. The obtained results have been shown in table (3). Based on the results presented, it is clear that the proposed method is not sensitive to unbalancing of load and feeder and accuracy of the method is satisfactory.

TABLE 2. The effect of the fault start angle on the precision of the proposed method.

Type of Fault	Fault Location (Node No.)	The fault start angle (grade) 0	45	90	170
		Errors Percentage			
A-g	2	0.0507	0.0507	0.0507	0.0507
	10	0.0433	0.0427	0.0427	0.0380
	8	0.0373	0.0347	0.0187	0.0680
AB	2	0.1600	0.1600	0.1600	0.1600
	10	2.2793	2.2793	2.2793	2.2793
	8	4.3980	4.3980	4.3980	4.3980
AB-g	2	0.2293	0.2413	0.2673	0.2900
	10	2.2453	2.3587	2.5993	2.8100
	8	4.1900	4.3980	4.8387	5.2260
ABC-g	2	0.0007	0.0067	0.0153	0.0007
	10	0.0060	0.0667	0.1467	0.0053
	8	0.0167	0.1320	0.2833	0.0153

TABLE 3. Evaluating the unbalanced distribution effect on the accuracy of the proposed method.

$R_F(\Omega)$	Fault Location (Node No.)	The type of the fault A-g	AB-g	AB	ABC-g
		Errors Percentage			
0	2	0.0107	0.0103	0.0101	0.0108
	10	0.0510	0.0506	0.0504	0.0512
50	2	0.9145	0.95418	0.9546	0.9541
	10	1.2040	1.2354	1.2415	1.2532

V. CONCLUSION

Techniques for locating faults play an important role in system recovery and repair. Therefore, many research works has been carried out on fault location in power transmission networks. However, due to the specification of the current distribution grids and equipment, it is difficult to use most of these techniques in practice. To cope with these, impedance-based techniques, mobile waves and intelligent techniques have been introduced for fault location in distribution networks. Unfortunately, these methods do not support fault location in four-wire power distribution networks. In this paper the impedance-based fault location technique is extended to support four-wire power distribution. The proposed method has been studied both theoretically and with numerical examples. The results show that the proposed technique is precise.

REFERENCES

[1] A. D. Filomena, M. Resener, R. H. Salim, and A. S. Bretas, "Distribution systems fault analysis considering fault resistance estimation," *Int. J. Elect. Power Energy Syst.*, vol. 33, no. 7, pp. 1326–1335, Sep. 2011.
[2] M.-S. Choi, S.-J. Lee, D.-S. Lee, and B.-G. Jin, "A new fault location algorithm using direct circuit analysis for distribution systems," *IEEE Trans. Power Del.*, vol. 19, no. 1, pp. 35–41, Jan. 2004.
[3] S.-J. Lee *et al.*, "An intelligent and efficient fault location and diagnosis scheme for radial distribution systems," *IEEE Trans. Power Del.*, vol. 19, no. 2, pp. 524–532, Apr. 2004.

[4] R. M. Ciric, L. F. Ochoa, A. Padilla-Feltrin, and H. Nouri, "Fault analysis in four-wire distribution networks," *IEE Proc.-Generat., Transmiss. Distrib.*, vol. 152, no. 6, pp. 977–982, Nov. 2005.
[5] H. Nouri and M. M. Alamuti, "Comprehensive distribution network fault location using the distributed parameter model," *IEEE Trans. Power Del.*, vol. 26, no. 4, pp. 2154–2162, Oct. 2011.
[6] S. Das, N. Karnik, and S. Santoso, "Distribution fault-locating algorithms using current only," *IEEE Trans. Power Del.*, vol. 27, no. 3, pp. 1144–1153, Jul. 2012.
[7] M. Daisy and R. Dashti, "Single phase fault location in electrical distribution feeder using hybrid method," *Energy*, vol. 103, pp. 356–368, May 2016.
[8] R. Dashti and J. Sadeh, "Applying dynamic load estimation and distributed-parameter line model to enhance the accuracy of impedance-based fault-location methods for power distribution networks," *Electr. Power Compon. Syst.*, vol. 41, no. 14, pp. 1334–1362, Sep. 2013.
[9] R. Dashti and J. Sadeh, "Fault section estimation in power distribution network using impedance-based fault distance calculation and frequency spectrum analysis," *IET Generat., Transmiss. Distrib.*, vol. 8, no. 8, pp. 1406–1417, Aug. 2014.
[10] J. Grainger and W. Stevenson, Jr., *Power System Analysis*. New York, NY, USA: McGraw-Hill, 1994.
[11] R. H. Salim, M. Resener, A. D. Filomena, K. R. C. de Oliveira, and A. S. Bretas, "Extended fault-location formulation for power distribution systems," *IEEE Trans. Power Del.*, vol. 24, no. 2, pp. 508–616, Mar. 2009.

RAHMAN DASHTI was born in Bushehr, Iran, in 1982. He received the B.Sc. degree from Shiraz University, Shiraz, Iran, in 2004, the M.Sc. degree from the Iran University of Science and Technology, Tehran, Iran, in 2006, and the Ph.D. degree in power electrical engineering from the Ferdowsi University of Mashhad, Iran, in 2013. He is currently an Assistant Professor and the Leader of the Power System and Protection Laboratory, Electrical Engineering Department, Faculty of Engineering, Persian Gulf University, Bushehr. His research interests include distribution systems, the protection and control techniques of distribution systems, fault location, and transient signal analysis.

MOHAMMAD DAISY was born in Bushehr, Iran, in 1984. He received the B.Sc. degree from Azad University, Bushehr, in 2012, and the M.Sc. degree from Persian Gulf University, Bushehr, in 2015. He is currently pursuing the Ph.D. degree in power electrical engineering from Islamic Azad University Central Tehran Branch. His research interests are distribution systems, protection and control techniques and fault location, power quality, and renewable energy.

HAMID REZA SHAKER received the Ph.D. degree from Aalborg University, Denmark, in 2010. He was a Visiting Researcher at MIT, a Post-Doctoral Researcher and an Assistant Professor at Aalborg University from 2009 to 2013, and an Associate Professor at the Norwegian University of Science and Technology, Norway, from 2013 to 2014. He is currently an Associate Professor at the Center for Energy Informatics, University of Southern Denmark. He is the leader of fault detection and diagnosis and processes monitoring research activities in the center. His contributions have been reported in more than 80 journal and conference publications. He serves three journals as a member of editorial board and has been an IPC member for several conferences.

MARYAMSADAT TAHAVORI received the Ph.D. degree from Aalborg University, Denmark, in 2014. She was a Visiting Researcher at Imperial College London and a Researcher at the University of Southern Denmark from 2013 to 2014. She is currently an Assistant Professor with the Center for Energy Informatics, University of Southern Denmark. Her contributions have been reported in several journal and conference publications. She has been an IPC member for several conferences.